RESEARCH PAPER

Polymeric nanoparticles containing 4-methoxychalcone attenuates hyperglycemia in diabetes-induced mice

Leonard Domingo Rosales Acho[1], Serafim Florentino Neto[1], Angela Maria Comapa Barros[1], Rosivaldo dos Santos Borges[2], Breno N. Matos[3], Tatiane Pereira de Souza[1], Guilherme Martins Gelfuso[3], Jesús Rafael Rodriguez Amado[4], Morteza Golbashirzadeh[5], Emersom Silva Lima[1]*

[1]Faculty of Pharmaceutical Sciences, Federal University of Amazonas, Manaus, AM, Brazil
[2]Institute of Health Sciences, Federal University of Pará, Belém, PA, Brazil
[3]Laboratory of Medicine, Food and Cosmetic Technology, University of Brasilia, Brasilia, DF, Brazil
[4]Faculty of Health Sciences, Federal University of Grande Dourados, Dourados, MS, Brazil
[5]Department of Pharmaceutical Biotechnology, Chabahar University of Medical Science, Chabahar, Iran

ABSTRACT

Objective(s): Diabetes mellitus is a chronic metabolic disorder characterized by persistent disturbances in glucose homeostasis. Novel therapeutic strategies are needed to improve glycemic control while minimizing toxicity. This study investigated the hypoglycemic potential of 4-methoxychalcone (MPP), synthesized via the Claisen–Schmidt reaction, and evaluated the efficacy of its nanoencapsulation in diabetic mice.

Materials and Methods: MPP was synthesized and subsequently nanoencapsulated (NCs) using ethanol, isopropyl palmitate, and organic phase surfactants. Nanocarriers were characterized by particle size, polydispersity index (PDI), zeta potential, and morphology through transmission electron microscopy (TEM). Diabetes was induced in CL57/6BL mice using streptozotocin/nicotinamide. Animals were treated for 28 days with free MPP (200 mg/kg), metformin (200 mg/kg), or NCs (10 mg/kg). Biochemical assays were performed on blood samples, and histological analyses were conducted on liver tissues.

Results: NCs exhibited a mean particle size of 187 nm, zeta potential of −19.9 mV, and PDI of 0.21, demonstrating stability across varying temperatures and pH conditions. TEM confirmed spherical morphology and uniform distribution. Both metformin (176.33 ± 44.68 mg/dL, $p < 0.0001$) and NCs (163.2 ± 76.3 mg/dL, $p < 0.0001$) significantly reduced blood glucose levels. NCs further normalized glycated hemoglobin (HbA1c) without evidence of hepatotoxicity, as indicated by low malondialdehyde levels and preserved liver histology.

Conclusion: Nanoencapsulation of MPP enhances its antidiabetic efficacy, enabling therapeutic effects at lower doses while reducing toxicity risks. This strategy represents a promising approach for the development of safer and more effective antidiabetic interventions.

Keywords: *Diabetes mellitus; Glycated hemoglobin; Hypoglycemic agents; Mice; Nanocapsules.*

How to cite this article

Acho LDR, Neto SF, Barros AMC, Borges RS, N. Matos B, de Souza PT, Gelfuso GM, Amado JRR, Golbashirzadeh M, Lima ES. Polymeric nanoparticules containing 4-methoxychalcone attenuates hyperglycemia in diabetes-induced mice. Nanomed J. 2026; 13(1): 159-169. DOI:10.22038/NMJ.2025.89217.2260.

INTRODUCTION

Diabetes mellitus is considered a metabolic syndrome whose main characteristic is chronic hyperglycemia, which is usually caused by some alteration in insulin receptors or by a drastic reduction in the production of this hormone [1,2]. It causes several complications, such as nephropathy [3,4], liver disease [5,6], immunodeficiency [7] and heart failure [8,9,10], among others that can affect two-thirds of diabetes sufferers [11,12]. Peripheral diabetic neuropathy affects half of the diabetic population [13]. For these reasons, diabetes and its complications cause serious socio-economic problems for families who have to deal with this disease on a day-to-day basis. In addition, in 2021, there was a global expenditure of approximately US$ 966 billion on diabetes patients, equivalent to 11.5% of all health spending [14].

* *Corresponding author:* Emersom Silva Lima, Professor, Faculty of Pharmaceutical Sciences, Federal University of Amazonas, Av. Gen. Rodrigo Otavio, 6200, CEP 69077-000, Manaus, AM, Brazil. E-Mail address: eslima@ufam.edu.br.

Note. This manuscript was submitted on July 03, 2025; approved on November 25, 2025.

Although current pharmacological therapies for glycemic control are efficient, they bring several adverse effects, such as weight gain, hypoglycemia, abdominal discomfort, diarrhea, nausea, vitamin B12 deficiency, risk of lactic acidosis, water retention and anemia, among others [15]. When insulin is injected under the skin, this can cause skin trauma with the formation of nodules; in addition, the body can produce antibodies to insulin, thereby requiring higher doses. Moreover, the cost of an insulin pump is high, and some patients do not respond to injections [16].

Given the problems related to diabetes treatments, there is a need to seek new therapeutic alternatives, intensified by the global increase in cases and treatments with clinical limitations [17]. Among these, testing innovative biovehicles such as nanoparticles, which are already described in the literature and demonstrate advantages, one of which is transporting promising molecules that are insoluble in water [18], which could modulate glucose metabolism. Within the group of chalcones we can highlight the presence of 4-methoxychalcone (MPP), which has demonstrated several interesting *in vitro* biological activities such as anti-inflammatory [19], glucose uptake stimulation [20], antineoplastic [21] and antitumor [22]. Although 4-methoxychalcone is more focused on innovative and selective antimitotic action [23]. It nevertheless presents chemical structures of chalcones at its base, which may contribute to enormous antidiabetic potential, acting on multiple pharmacological targets (PPARγ, α-glicosidase, PTP1B) [24, 25].

Although the MPP molecule has demonstrated interesting biological activities, it has one main disadvantage, it is insoluble in water, making it not very useful orally and limiting its absorption. In addition, it is necessary to use high amounts of MPP to achieve the desired pharmacological effect, which could cause difficulties in its bioavailability. These disadvantages have made the molecule unattractive in the eyes of researchers looking for new treatments for diabetes and its complications [26]. Both 4-methoxychalcone (MPP) and the sulfonamide chalcone derivative IP-004 display antidiabetic activity; nevertheless, both compounds show poor oral absorption. In diabetic murine models, treatment with IP-004 via intraperitoneal injection at 20 mg/kg significantly lowered circulating glucose concentrations. [27]. Although MPP also stimulates glucose uptake *in vitro*, its high lipophilicity limits aqueous solubility and, consequently, intestinal absorption [19].

Studies using nanotechnology have shown that the average size of nanocarriers can result in an improvement in the therapeutic activity of drugs. The application of this technology signifies a differentiated profile for the release of drugs, such as nanocapsules, which can achieve positive results in both distribution, specificity, and/or penetration of substances into tissues. The influence on absorption is one of the fundamental advantages of nanopharmacology [18].

Given the above context, the present study aimed to develop a nanodispersed polymeric system containing MPP, then evaluate its effect on the glycemia of diabetic mice and investigate its toxicity. Our objective was achieved by establishing technically stable nanocapsules incorporated with MPP as a prototype for diabetes treatment, oral route of administration.

MATERIALS AND METHODS

Chemicals

The inputs utilized in the development of the nanocapsules were MAE 100 P (Kollicoat®), Sorbitan monolaurate (Span®20), polyoxyethylene sorbitan monooleate (Tween®80), and isopropyl palmitate (PMP). Streptozotocin (STZ) and nicotinamide (NA), required for in vivo assays, were obtained from Sigma-Aldrich (St. Louis, MO, USA). The kits used for the biochemical analyses were from Wiener Lab (Rosario, Argentina). As for the MPP, this was quantified synthetically and presented 96.32% purity according to a study of [28].

Synthesis of 4-methoxychalcone (MPP)

For the synthesis of MPP, the Claisen-Schmidt condensation method was used [29], using p-methoxy-benzaldehyde [30] and acetophenone [31] as reagents (0.12 and 0.1 eq., respectively). Transformation of the aromatic aldehyde into chalcone (MPP) was achieved by exposure to 0.05 eq. NaOH in a mixed ethanol–water solvent system, with the reaction conducted at temperatures not exceeding 10 °C. The compound was purified by recrystallization and identified using mass spectra analysis and nuclear magnetic resonance of hydrogen and carbon.

Preparation of the nanocapsules

The nanoencapsulation of the MPP was performed following the solvent displacement method described by [32] under constant stirring at 400 rpm for 30 min at room temperature, carried out in two phases (Table 1). The organic phase contained isopropyl palmitate, MPP, Span® 20, Kollicoat®, 96% ethanol, and acetone. The aqueous phase was composed of ultrapure water and Tween® 80. The incorporation of the nanocapsule with the MPP was through the junction of the

organic phase by dripping on the aqueous phase that remained under agitation. After complete stirring of the formulation, it was left top stand for 20 minutes, then it was homogenized in a blender (Ultra-turrax® IKA, Switzerland) at 10xg for 10 min to obtain particles of viable sizes. At the end of the process, alcohol and acetone were eliminated using vacuum rotary evaporation (IKA, Switzerland) at 50°C.

Size and PDI

The calculation of particle size and polydispersity index (PDI) was conducted using photon correlation spectroscopy (PCS) with a Zetasizer Nano (Malvern, USA), operating at 633 nm wavelength, 173° scattering angle, and 25 °C [33]. The nanocapsule formulation was pre-filtered through a Millipore® membrane (0.45 µm) before measurement. Triplicate determinations were conducted, from which the mean and standard deviation were subsequently derived.

Zeta potential and conductivity

The determination of zeta potential and conductivity was carried out using a Zetasizer particle size analyzer (Malvern, USA) fitted with a disposable polycarbonate zeta cell. Electrophoretic mobility measurements were automatically transformed into zeta potential values using the Smoluchowski approximation. Measurements were conducted at 25 °C under an applied voltage of 150 V, a parameter integrated into the instrument's software to calculate zeta potential from electrophoretic mobility [33]. Each sample was analyzed in triplicate, and mean values with standard deviations were reported.

Effect of pH

The influence of pH on nanocapsule size and zeta potential was assessed using an MPT-2 titrator (Malvern, UK) coupled to a Zetasizer particle size analyzer. Titrations were performed with sodium hydroxide (0.1 mol/L) and hydrochloric acid (0.1 mol/L). Instrument calibration was carried out with buffer solutions at pH 4, pH 7, and pH 10 (Alphatec, Brazil). Triplicate measurements were conducted for all experiments under standardized conditions at 25 °C[34].

Thermal effect

The effect of temperature on nanocapsule particle size and polydispersity index was investigated by subjecting the suspension to heating between 20 °C and 70 °C, at 5 °C increments. Samples were equilibrated for 5 minutes at each temperature prior to measurement. Triplicate determinations of particle size and PDI were obtained, and values were presented as mean with standard deviation [34].

Morphology

Transmission electron microscopy (JEM 1011, Tokyo, Japan) was utilized to acquire morphological images of the nanocapsules. The samples were diluted in water (1:200, v/v), mounted on gold grids, coated with formvar resin, and air-dried at ambient temperature. Residual formulation was removed using filter paper. A 3 µL aliquot of 3% (w/v) uranyl acetate was subsequently added and dried for 5 minutes at room temperature in the absence of light. Morphological assessment was conducted at magnifications of 10,000× and 25,000×.

In vivo study

For this study, male Swiss mice (Unib:SW), six weeks of age and weighing 18–20 g, were obtained from the Central Animal Husbandry Unit at UFAM, Manaus. The animals were maintained under standardized laboratory situations, with a 12-h light/dark cycle, measured temperature of 21 ± 1 °C, and relative humidity of 35–60%. They were provided with standardized vivarium feed and water ad libitum[35].

Induction of diabetes

Diabetes induction was achieved according to the protocol designated in [36] with minor adaptations. Animals received nicotinamide (50 mg kg^{-1} body weight) diluted in saline, followed 20 minutes later by intraperitoneal administration of streptozotocin (150 mg kg^{-1} body weight) prepared in 0.1 M citrate buffer at pH 4.5. After 96 hours, animals presenting blood glucose levels above 200 mg/dL were classified as diabetic.

DM2 chronic hypoglycemic activity test

Diabetic mice were randomly divided into seven groups, with each group containing six animals. The groups were alienated as follows: 1) non-diabetic group (normoglycemic) (NG); 2) untreated diabetic group (DG); 3) group treated with metformin 200 mg kg^{-1} (GP200) per animal, orally; 4) group treated with MPP, with 100 mg kg^{-1} (MPP100) per animal, orally; 5) group treated with MPP, with 200 mg kg^{-1} (MPP200) per animal, orally; 6) group treated with nanocapsules containing MPP, with 5 mg kg^{-1} (NC5) per animal, orally; 7) group treated with nanocapsules containing MPP, with 10 mg kg^{-1} (NC10) per animal, orally.

Every seven days, sufficient time to monitor treatment progress without causing unnecessary pain or stress to the animals, blood glucose was measured and the groups were weighed. Blood glucose was measured using a Precision Xtra glucometer (Abbott Diabetes Care, Portugal) by placing a small drop of blood on a new test strip and the measurements were recorded. Treatment was started after the confirmation of diabetes [36].

Blood and liver collection after the chronic test

At the end of the treatment, the animals were anesthetized intraperitoneally with ketamine and xylazine (100:10 mg/kg bw). Blood was collected via cardiac puncture to measure biochemical parameters, then euthanasia was performed by cervical displacement. After exploratory laparotomy, the liver was sectioned and placed in a 10% formalin solution buffered to pH 7 for further histological analysis. In addition, malonaldehyde was dosed with 1 g of liver fragments that were stored at -70^{o}C in 10 mL of phosphate buffer pH 7 until the day of the test.

Biochemical analysis

At the end of the treatment, after euthanasia, whole blood was collected by intracardiac puncture with the aid of a heparinized syringe. After separation of plasma by centrifugation, this was used to determine the glycemic (glucose and HbA1c), lipid (cholesterol and triglycerides), hepatic (ALT and AST) and renal (uric acid, creatinine and urea) profiles. The levels were determined using an automatic analyzer (Chem Well Model 2910; Awareness Technology Inc) and Wiener Lab biochemical and ELISA commercial Kits (Wuhan Fine Biological Technology) [35].

Dosage of malonaldehyde (MDA)

Hepatic malondialdehyde (MDA) levels were quantified using the thiobarbituric acid reactive substances (TBARS) assay, which estimates lipid peroxidation intensity through the formation of a pink chromogen. In short, a 1 g portion of liver tissue was homogenized in 10 mL of 150 µM NaCl. An aliquot of 100 µL homogenate was added to 1.5 mL of reaction mixture comprising 0.1% thiobarbituric acid, 0.25 N hydrochloric acid, and 10% trichloroacetic acid. Samples were vortexed for 30 s, sealed with marbles, and incubated in a water bath at 100 °C for 45 min. Next, centrifugation at 3.5×g for 5 min, the supernatant was analyzed at 535 nm using a UV/VIS spectrophotometer (T70, PG Instruments Ltd). Results were expressed in µmol/L of MDA, based on a calibration curve prepared with 1,1,3-tetrahydroxypropane standards at 0.25, 0.5, 1.0, 2.0, 4.0, and 8.0 µmol [37].

Histological analysis

Liver and kidney tissue samples from each mouse were sequentially dehydrated in graded concentrations of ethyl alcohol (70%, 80%, 96%, and 100%), followed by immersion in xylol/alcohol (1:1) and subsequently in 100% xylol for 30 minutes each. All samples were fixed in paraffin blocks at 60 °C and maintained under refrigeration. Slices of 3–5 µm thickness were produced with a microtome (RM 2125rt, Leica Microsystems, Wetzlar, Germany), mounted on slides, stained with hematoxylin and eosin (HE), and fixed with Canada balsam. Coverslips were used, and the samples were examined under a DM500 optical microscope (Leica Microsystems, Wetzlar, Germany) fitted with an ICC50W integrated camera.

Statistical analysis

To show the differences between the groups analyzed *in vivo*, one-way ANOVA for univariate results and two-way ANOVA and Dunnett's test for bivariate results were used for analysis, with $P < 0.05$ being measured statistically important. Analysis was reached using the software GraphPad Prism®.

RESULTS AND DISCUSSION

Size, PDI, and Zeta potential

The size of the nanocapsules of the formulation showed an average diameter of 187.0 ± 3.8 nm and maintained a narrow monomodal distribution with a PDI of 0.210 ± 0.007, as shown in Fig. 1A.

The developed nanoparticles had a zeta potential of -19.0 ± 0.7 mV, which did not change over time (Fig. 1B). As for conductivity, the measurement was 0.041 ± 0.004 m/s cm^{-1}. The particles presented a decreased mobility of free ions in the solution. Regarding the effect of pH on particle size (Fig. 1C), it was observed that at pH 5 the nanoparticles remained unchanged, suffering small variations in size when exposed to a pH above 6, with rupture of the particles at pH 9. However, the stability of the particles at pHs below 5 indicated that the nanocapsules may be gastro-resistant. On the other hand, the isoelectric point of the zeta potential increased between pH 1 and 5, accentuating at pH 9 and reaching a value of -40 mV, which may favor the release of the active ingredient in the intestine. The results obtained in these tests may indicate that the nanocapsules should not undergo major structural changes at pH values of less than 5.

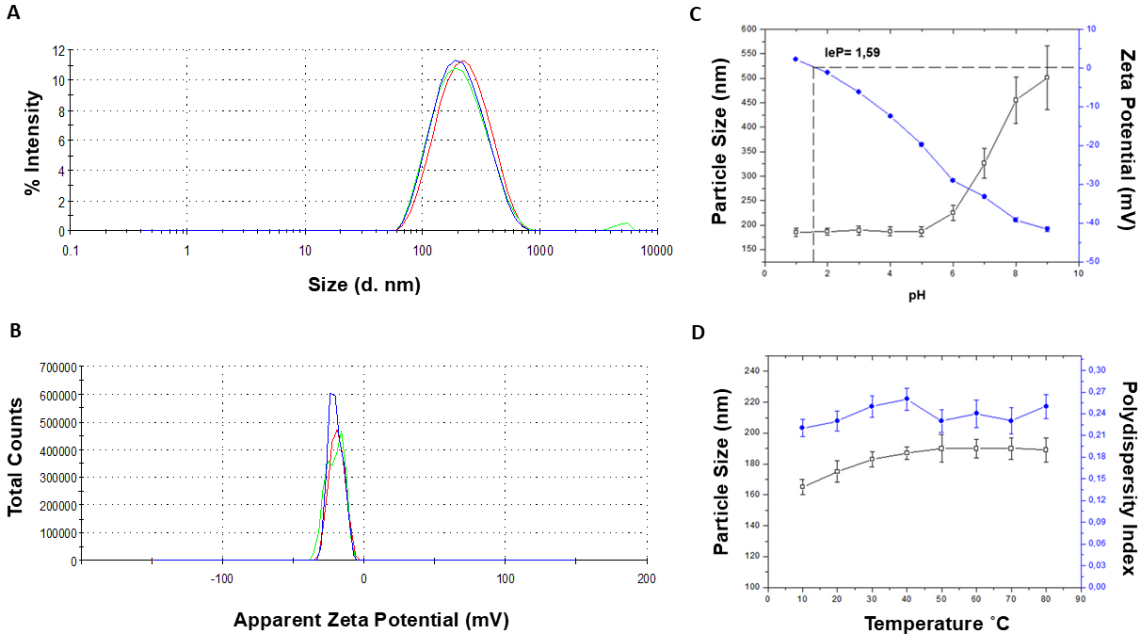

Fig. 1. Size and distribution of nanocapsules (A); zeta potential (B); effect of pH on the zeta potential of the nanocapsules (C); effect of temperature on particle size and dispersion index of nanocapsules (D).

As for the effect of thermal stability, this is shown in Fig. 1D. The result obtained was within what is expected for this type of molecule, with melting temperatures between 10 to 70°C. With regard to the particle size and the polydispersity index, the variation in particle size remained between 160 and 180 nm. The polydispersity index remained between 0.240 and 0.260, which indicate the high thermal stability of the nanocapsules.

The average diameter of the particles and their homogeneous distribution are of paramount importance for their biological activity, as these parameters can influence their biodistribution and blood clearance [38]. Polystyrene nanoparticles coated with D-α-tocopheryl polyethylene glycol (TPGS) at sizes of 100 and 200 nm demonstrated the potential to encapsulate drugs and deliver them through the gastrointestinal or blood-brain barrier [39]. In addition, each formulation may contain a particular point of surface or repulsion force between the particles [40]. High zeta potential values, over 30 mV, positive or negative, suggest more stable nanocapsules suspensions, due to the repulsion between the particles that prevents their aggregation [41]. However, the study showed a zeta potential value of -19 mV, indicating moderate stability of the formulation at a pH of up to 5.

Morphology

The nanocapsules exhibited a spherical shape and showed no sign of agglomeration. Their size range is consistent with that observed by DLS analysis. Additionally, electron micrographs confirmed the nanocapsules' relatively uniform and monomodal distribution (Fig. 2) end composition in Table 1).

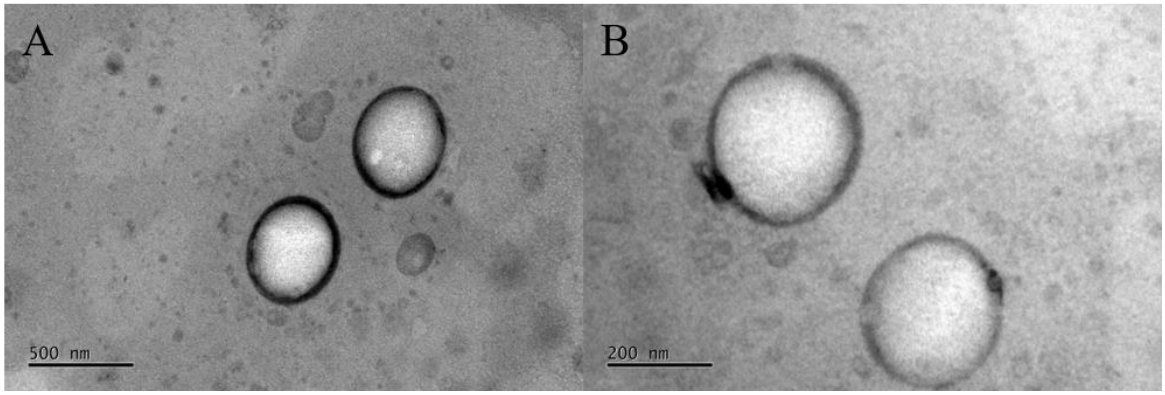

Fig. 2. Electron micrographs obtained using TEM to analyze the morphology and size range of the nanocapsules (A: 10,000 ×, B: 25,000 ×).

Table 1. Composition of nanocapsules containing MPP

Organic phase	Minimum	Maximum	Ideal
Isopropyl palmitatate (mg)	300	800	500
MPP (mg)	25	100	50
Span® 20 (mg)	300	1.000	500
Kollicoat® MAE 100P (mg)	100	1.000	350
Ethanol 96% (ml)	5	20	5
Acetone (ml)	5	50	15
Aqueous phase			
Tween® 80 (mg)	100	800	500
Ultrapure water (ml)	25	100	50

The development and stability of the nanoparticles were due to the combination of two nonionic surfactants (Span® 20 and Tween® 80), which maintained the particle size practically constant for extended periods, enhancing medium stability and preventing aggregate formation during storage [37,42].

Similar results were observed in this study. The study by [34], investigated Kollicoat® MAE 100P, which is a versatile polymer, and one that can be used for the preparation of gastro-resistant nanoparticles with drugs of various origins. The use of this polymer represents a viable, low-cost, and multifunctional alternative for the preparation of nanoparticle systems. Furthermore, in the intestine, Kollicoat® MAE 100P enables a slower release of MPP, dissolving gradually in environments with pH >5.5 and achieving complete dissolution within 90 minutes. Nanocapsules are usually used as carriers of poorly soluble drugs to recover stability and/or bioavailability [43].

To date, there are no specific reports addressing the nanoencapsulation of MPP. Kollicoat® MAE 100P was selected due to its proven biocompatibility, pH-dependent solubility, and ability to protect bioactive molecules from gastric degradation while enabling controlled intestinal release. Moreover, its excellent film-forming properties and moderate stability make this polymer particularly suitable for improving the oral absorption of highly lipophilic compounds such as MPP. The choice of Kollicoat® MAE 100P was also based on the study by [44], who successfully employed this polymer in the formulation of nanocapsules containing amirenone, a molecule with high lipophilicity.

Our formulation was developed based on the approach described by [44], while the specific proportions were optimized experimentally in our laboratory. However, detailed formulation parameters cannot be disclosed in the manuscript, as they are part of an ongoing patent application. We emphasize that all experimental conditions were standardized and reproducible, ensuring the reliability and consistency of the results presented.

In vivo study

Treatment with MPP and MPP-loaded nanocapsules for 7 weeks significantly reduced blood glucose levels in diabetic mice when compared to the diabetic control group (469.5 ± 131.8 mg/dL), with blood glucose decreasing to 246.2 ± 39.4 mg/dL (MPP200), 197.3 ± 91.9 mg/dL (NC5), 163.2 ± 76.3 mg/dL (NC10), and 176.3 ± 44.7 mg/dL (MET200). These effects persisted throughout the treatment period (Figs. 3A and 3B), demonstrating a sustained hypoglycemic action of the nanoformulations.

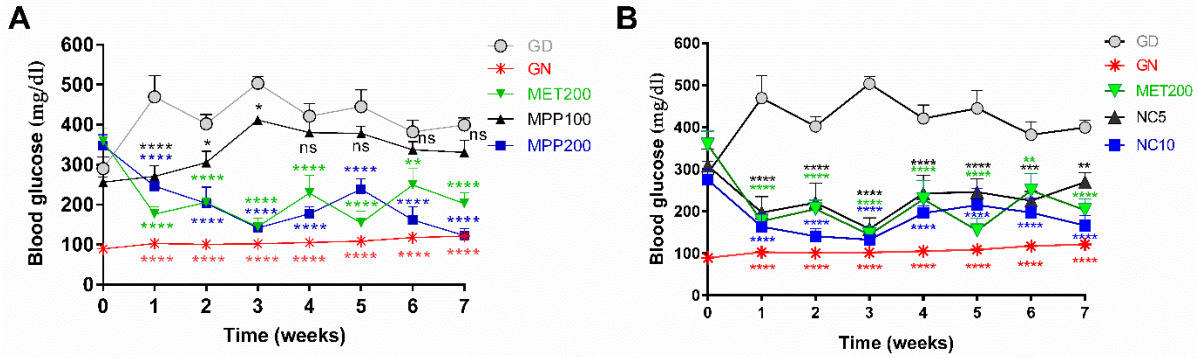

Fig. 3. Glycemic levels of diabetic mice after 7 weeks of treatment with MPP or nanocapsules containing MPP. Mice with glycemia greater than 200 mg/dL were separated and divided into groups: non-diabetic group (NG), untreated diabetic group (DG), metformin 200 mg kg^{-1} (GP200) and groups treated with MPP 100 mg kg^{-1} (MPP100) and 200 mg kg^{-1} (MPP200) are shown in Figure 3A; groups treated with nanocapsules containing MPP 5 mg kg^{-1} (NC5) and 10 mg kg^{-1} (NC10) are shown in Figure 3B. Values are expressed as mean ± SEM for (n = 6) with analysis using two-way ANOVA for multiple comparisons and Dunnett's test. Asterisks represent statistical differences - $p < 0.05$ **$p < 0.01$; *** $p < 0.001$; **** $p < 0.0001$ and $^{ns}p > 0.05$ shows no statistical difference.

Table 2. Results of biochemical parameters of mice treated for seven weeks

	Cholesterol Mg/dL	Triglycerides Mg/dL	Creatinine Mg/dL	Urea Mg/dL	Uric Acid Mg/dL	TGO U/L	TGP U/L
NG	87±9 [a]	45±16 [a]	0.3±0.1 [a]	44±6 [a]	1±0.2 [a]	22±12 [a]	23±12 [a]
DG	86±12 [a]	68±17 [a]	1.1±0.3b	79±15bc	2±0.7 [bc]	20±11 [a]	20±11 [a]
MET200	96±17 [a]	64±25 [a]	1.4±0.6b	42±19 [ac]	1.5±0.4 [ac]	32±16 [a]	32±16 [a]
MPP200	77±18 [a]	38±22 [a]	0.32±0.17 [a]	51±9 [ac]	0.8±0.3 [a]	22±11 [a]	22±11 [a]
MPP100	93±22 [a]	50±28 [a]	0.9±0.17 [a]	57±26 [ac]	1.4±0.5 [ac]	23±13 [a]	23±13 [a]
NC10	76±17 [a]	49±14 [a]	0.27±0.07 [a]	46±20 [a]	0.8±0.6 [a]	11±6 [a]	26±13 [a]
NC5	81±9 [a]	47±7 [a]	0.29±0.04 [a]	46±14 [a]	0.4±0.5 [ad]	18±10 [a]	28±17 [a]

The values are expressed as mean ± SEM (n = 6) with analysis via two-way ANOVA for multiple comparisons and Dunnett's test. Different letters represent statistical differences - P < 0.05.

When the data are expressed as a percentage of improvement in diabetic control, the reductions correspond to 47.6% (MPP200), 58.0% (NC), 65.2% (NC10), and 62.5% (MET200). These quantitative comparisons demonstrate that MPP at 200 mg·kg^{-1} exerts a hypoglycemic effect comparable to that of metformin, while the nanoencapsulated forms, in particular NC10, potentiated this therapeutic response. These findings reinforce the enhanced efficacy of MPP when administered via nanocapsules, likely due to better bioavailability and sustained release of the active compound.

The study by [45] showed that the nanoparticles preserved the high antioxidant capacity of curcumin, as well as presented significant antimicrobial activity for bacteria, without presenting toxicity for normal cells, only being cytotoxic for cancer cells. Another study showed that α-amyrin-loaded nanocapsules showed excellent potency and efficacy as antileukemic agents, without presenting a cytotoxic effect in normal cells, which suggests a selective cytotoxicity against leukemia cells [44]. In the study by [46], the researchers investigated a nanoparticle system loaded with ellagic acid (EA), a compound with antiproliferative activity stemming from its ability to inhibit the binding of carcinogens and specific nitrosamines to DNA. However, therapeutically, EA exhibits low aqueous solubility and bioavailability, resulting in minimal therapeutic benefit and limiting its full clinical application. The study concluded that the nanoparticles remained stable for over 24 hours, with *in vitro* drug release exceeding 80%, which could improve dosing frequency and support their potential use in future research in the field of oral oncology.

Through the biochemical results shown in (Table 2), it can be observed that cholesterol and triglycerides did not present statistical differences between the groups studied. The parameters of creatinine levels showed damage in the MET200 and DG groups, while urea and uric acid levels showed damage in the DG group, and a slight damage in the MET200, MPP100 and MPP200 groups. The liver biochemical parameters ALT and TGP showed homogeneous results between the groups.

Biochemical parameters are widely used as physiological indicators of animals in response to endogenous changes and as diagnostic biomarkers. Changes in these parameters may suggest, for example, injuries to specific organs or tissues, assist in the toxicological evaluation of drug candidates, and detect deficiencies in the species' rearing system [47]. In this study, it was observed that the NC10 and NC5 nanoparticles didn't cause hepatic damage.

Regarding glycated hemoglobin (HbA1c) levels, the MPP200 group presented a mean value of 4.5 ± 0.4% and the NC10 group a mean value of 4.6 ± 0.4%. These values were similar to the negative control group, for which the value was 4.3 ± 0.2%, which is much lower than the untreated group, since HbA1c levels were 7.4 ± 0.3%. These experimental treatments were shown to be more effective in inhibiting hemoglobin glycation than metformin 200 mg kg^{-1} pc (6.1 ± 1%), as shown in Fig. 4.

The high concentration of malonaldehyde (µmol/g) shown in Fig. 5, demonstrated liver damage of group MPP100 (3.4 ± 0.6) when compared with NG group (5.5 ± 1.8). MPP200 (0.9 ± 0.1) and NC10 (1.1 ± 0.1) did not show oxidative liver damage in relation to the NG group. The MET200 (1.9 ± 0.1) and NC5 (2 ± 1) groups showed a slight increase in malonaldehyde when compared with GN group.

Intrinsic and extrinsic stimuli can provoke excessive and sustained production of reactive oxygen species (ROS) beyond physiological metabolic levels, potentially damaging cellular structures, enhancing lipid peroxidation, impairing function, and weakening immune responses [48]. This oxidative imbalance produces lipid hydroperoxides and aldehydes such as malondialdehyde, 4-hydroxynonenal, and isoprostanes, ultimately culminating in cell death [49]. Findings from this study revealed that nanocapsule-treated groups (NC10 and NC5) showed reduced malondialdehyde release compared to the untreated control group (NG).

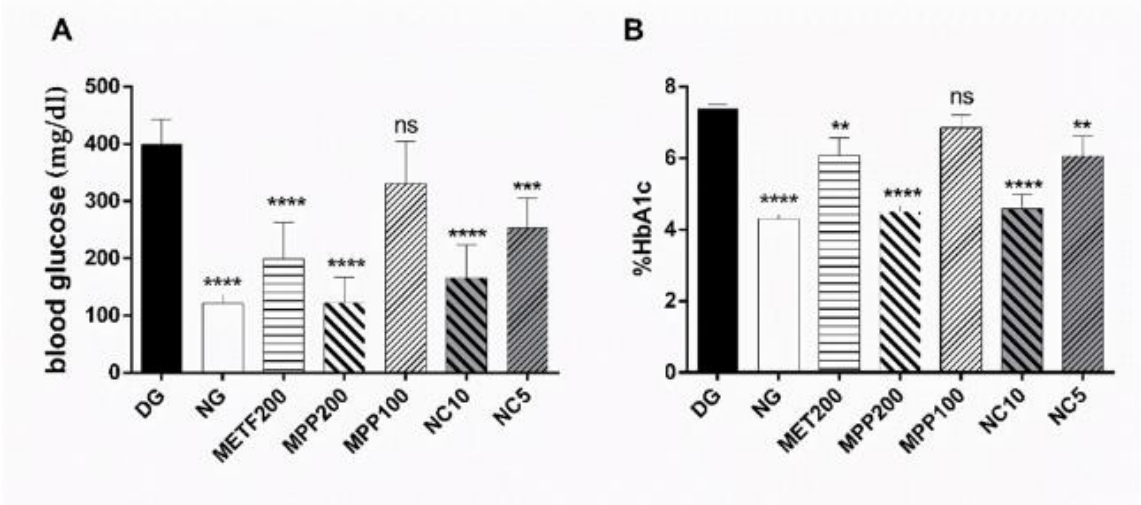

Fig. 4. Blood glucose (A) and glycated hemoglobin (B) levels in diabetic mice after seven weeks of treatment with MPP and MPP-containing nanocapsules. Values were expressed as mean ± SEM (n = 6). For the analysis, a two-way ANOVA was used. The treated groups were compared with the untreated diabetic group (DG) using Dunnett's test. Asterisks represent statistical differences - P < 0.05 **P < 0.01; *** P < 0.001; **** P < 0.0001 and ns P > 0.05 shows no statistical difference.

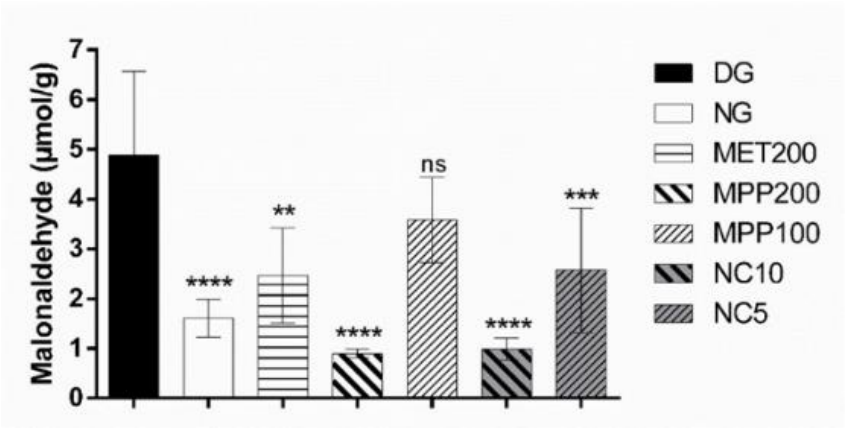

Fig. 5. Serum malonaldehyde levels in diabetic mice after seven weeks of treatment with MPP and nanocapsules containing MPP. Values were expressed as mean ± SD (n = 6). For the analysis, a two-way ANOVA of the treated groups was used. The treatment groups were compared with the untreated group (NG), using Dunnett's test. Asterisks represent statistical differences - P < 0.05 **p < 0.01; *** P < 0.001; **** P < 0.0001 and ns P > 0.05 shows no statistical difference.

After treatment of hyperglycemic animals with nanocapsules containing MPP, a glycated hemoglobin level of NC10 of 4.5% and a lower glucose value than the reference treatment were observed. These biochemical tests are one of the main diagnostic methods for hyperglycemia and diabetes used in clinical medicine, considered the gold standard [50], and were performed in this study. The MDA method in urine, although an important tool, is indicated for complicated diabetes management cases (screening for renal complications, detection of ketonuria and infections), and not for the diagnosis of hyperglycemia and diabetes [51]. Therefore, this study sought to track these complications from the liver, where MDA is metabolized and can cause cellular damage. However, it was observed that the NC5 and NC10 samples reduced MDA production, resulting in a possible neutralization of the molecule, corroborating the liver markers AST and ALT which were within normal limits.

In the histological analysis of the livers, the untreated group showed a normal architecture of hepatocytes (h) with narrow sinusoid capillaries (s), some binucleated hepatocytes and Kupffer cells (Fig. 6a). In the DG group, we have few hepatocytes (h) and all are hypertrophic expressing vascular reduction, presence of inflammatory infiltrate (inf), microvesicular infiltrate (hst) with droplets and glycogen and macrovesicular steatosis (yellow arrow) with well-defined fat droplets. There are also cells in apoptosis, with some Küpper cells, due to their low vascularization with dilated sinusoid (sd) capillaries. This group presents very marked and characteristic possible liver damage (Fig. 6d). In the MPP100 group, we can observe several

apoptotic hepatocytes (hap), with the presence of a predominant inflammatory infiltrate (inf) with dilated sinusoid capillaries and hepatocytes with microvesicular infiltrate (hst). This shows the presence of significant liver damage (Fig. 6e). The MPP200 (Fig. 6b) and NC10 (Fig. 6c) groups have a normal architecture without damage similar to the NG group, which was also indicated by a low production of malonaldehyde produced in this tissue. The NC05 group (Fig. 6f) had only one microvesicular steatosis (hst). These findings also corroborate the results of the MDA test.

The liver plays a pivotal role in metabolic regulation and in the detoxification and elimination of toxic compounds. Because of its extensive functional reserve, injury to this organ may not instantly affect its performance. Thus, tests reflecting hepatocellular injury, such as plasma liver enzyme measurements, are necessary. Yet, standard biochemical assays often lack diagnostic precision, making further investigations such as liver biopsy necessary to detect pathological changes [52]. The present study confirmed that NC10 and NC5 confer protection against diabetes-induced renal and hepatic damage.

CONCLUSIONS

The nanoformulation containing MPP exhibited medium-sized particles and moderate zeta potential stability up to pH 5, at temperatures ranging from 20 °C to 70 °C. Furthermore, coating the nanocapsules with Kollicoat® MAE 100P resulted in a delayed release of the bioactive compound at intestinal pH during a seven-week treatment in diabetic mice, leading to a promising antidiabetic effect of the developed formulation, superior to the non-encapsulated form. Additionally, the nanocapsules containing MPP at a dose of 10 mg kg^{-1} did not exhibit hepatic or renal toxicity. Therefore, the nanoencapsulation system demonstrated antidiabetic activity *in vivo*. However, further pharmacokinetic investigations of nanoformulation are necessary.

ACKNOWLEDGMENTS

Not applicable

CONFLICT OF INTEREST

The authors declare that there are no conflicts of interest, financial or otherwise.

FUNDING

The authors are grateful for the financial support received from the Government of the Amazonas State through the Fundação de Amparo à Pesquisa do Estado do Amazonas (FAPEAM), Coordenação de Aperfeiçoamento de Pessoal de Nível Superior (CAPES) and Conselho Nacional de Desenvolvimento Científico e Tecnológico (CNPq).

ETHICAL CONSIDERATIONS

The experimental protocol was based on the guidelines of the Brazilian National Council for Animal Experimentation Control (CONCEA) and approved by the Ethics Commission on the Use of Animals (CEUA) of the Federal University of Amazonas (UFAM) under protocol No. 004/2019.

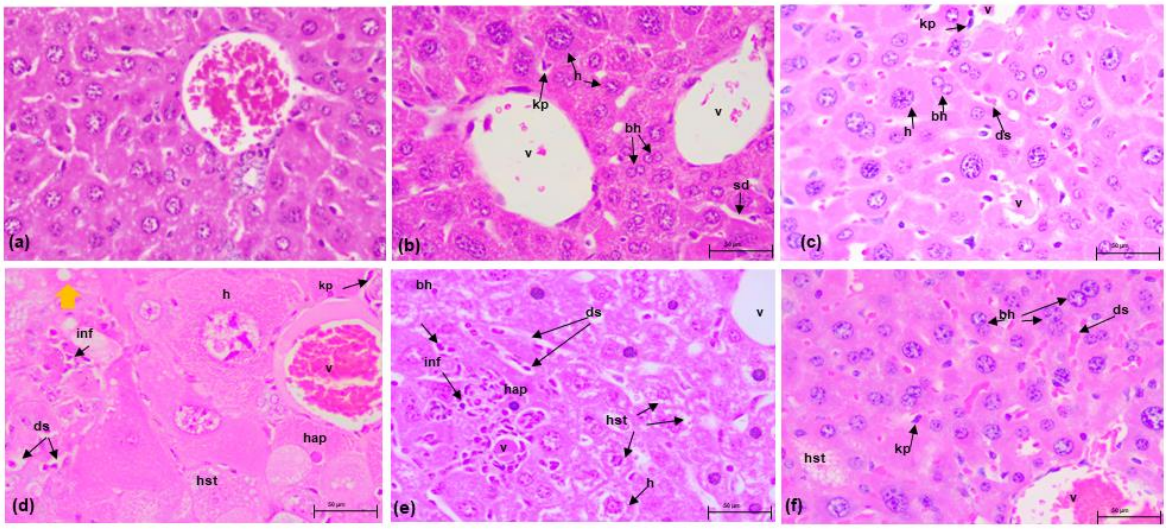

Fig. 6. Effect of treatment in streptozotocin-induced diabetic mice seen in liver histopathology determined via HE staining (400x magnification, 50 µm on bar scale). NG (a), DG (d), MPP200 (b), MPP100 (e), NC10 (c), NC5 (f) and MET 200 (g). h: hepatocyte; bh: bilateral hepatocyte; s: sinusoidal capillary; ds: dilated sinusoid; gc: glycogen content; Kp: Kupffer cell; hap: hepatocyte in apoptosis; hst: hepatocyte in microvesicular steatosis; inf: inflammatory infiltrate; yellow arrow: macrovesicular steatosis.

AUTHOR CONTRIBUTIONS

Leonard Domino Rosales Acho: Project development, data collection, statistical analysis, and manuscript writing; Serafim F. Neto: Data processing and manuscript writing; Angela Maria Comapa Barros: Data processing and critical revision; Rosivaldo dos S. Borges: Data processing and manuscript writing; Breno N. Matos: Data processing and manuscript writing; Tatiane Pereira de Souza: Data processing and critical revision; Guilherme M. Gelfuso: Data analysis; Jesús R. R. Amado: Data analysis; Emerson Silva Lima: Project coordination, data collection, and critical revision.

REFERENCES

1. Champe PC, Harvey RA, Ferrier DR. Bioquímica Ilustrada. 3ª ed. Porto Alegre (PA): Artmed; 2006.
2. Baynes JW, Dominiczak MH. Bioquímica Medica. 5ª ed. Rio de Janeiro (RJ): Elsevier; 2019.
3. Teng B, Duong M, Tossidou I, Yu X, Schiffer M. Role of protein kinase C in podocytes and development of glomerular damage in diabetic nephropathy. Front Endocrinol (Lausanne). 2014;5:5-179.
4. Yingnan F, Lau ESH, Wu H, Yang A, Chow E, So Asa-Yee, et al. Incidence of long-term diabetes complications and mortality in youth-onset type 2 diabetes: A systematic review. Diabetes Res Clin Pract. 2022;191:e110030.
5. Hamed AE, Elsahar M, Elwan NM, El-Nakeep S, Naguib M, Soliman HH, et al. Managing diabetes and liver disease association. Arab J Gastroenterol. 2018;19:166-179.
6. Hamed AE, Elwan N, Naguib M, Elwakil R, Esmat G, El Kassas M, et al. Diabetes Association with Liver Diseases: An Overview for Clinicians. Endocr Metab Immune Disord Drug Targets. 2019;19:274-280.
7. Meza LCE, San Martín OCA, Provoste JJr, Zaror CJF. [Pathophysiology of diabetic nephropathy: a literature review]. 2017;17:e6839.
8. Shah MS, Brownlee M. Molecular and Cellular Mechanisms of Cardiovascular Disorders in Diabetes. Circ Res. 2016;118:1808-1829.
9. Lehrke M, Marx N. Diabetes Mellitus and Heart Failure. Am J Med. 2017;130: S40-S50.
10. Ochoa-González FL, González-Curiel IE, Cervantes-Villagrana AR, Fernández-Ruiz JC, Castañeda-Delgado JE. Innate Immunity Alterations in Type 2 Diabetes Mellitus: Understanding Infection Susceptibility. Curr Mol Med. 2021;21:318-331.
11. Giacco F, Brownlee M. Oxidative stress and diabetic complications. Circ Res. 2010;107:1058-1070.
12. Pavlou DI, Paschou SA, Anagnostis P, Spartalis M, Spartalis E, Vryonidou A, Tentolouris N, Siasos G. Hypertension in patients with type 2 diabetes mellitus: Targets and management. Maturitas. 2018;112:71-77.
13. Smulyan H, Lieber A, Safar ME. Hypertension, Diabetes Type II, and Their Association: Role of Arterial Stiffness. Am J Hypertens. 2016;29:5-13.
14. Feldman EL, Callaghan BC, Pop-Busui R, Zochodne DW, Wright DE, Bennett DL, et al. Diabetic neuropathy. Nat Rev Dis Primers. 2019;5:41.
15. Brazilian Diabetes Society Guideline. Brazil: Brazilian Diabetes Society (SBD), 2019-2020. Available: https://www.saude.ba.gov.br/wp content/uploads/2020/02/Brazilian-Diabetes-Society-Guidelines -2019-2020.pdf
16. Chantelau E, Lange G, Sonnenberg GE, Berger M. Acute cutaneous complications and catheter needle colonization during insulin pump therapy. Diabetes Care. 1987;10:478-482.
17. Aloke C, Egwu CO, Aja PM, Obasi NA, Chukwu J, Akumadu BO, et al. Current Advances in the Management of Diabetes Mellitus. Biomedicines. 2022;10:2436.
18. Apolinário AC, Salata GC, Bianco AFR, Fukumoria C, Lopes LB. Opening the pandora's box of nanomedicine: there is indeed plenty of room at the bottom. Quim Nova. 2020;43:212-225.
19. Hsieh CT, Hsieh TJ, El-Shazly M, Chuang DW, Tsai YH, Yen CT, et al. Synthesis of chalcone derivatives as potential anti-diabetic agents. Bioorg Med Chem Lett. 2012;22: 3912-3915.
20. Federação Internacional de Diabetes. Diabetes Atlas, (10ª ed. Bruxelas). 2024. Available: https://www.diabetesatlas.org. https://diabetesatlas.org/atlas/tenth-edition/
21. Shih TL, Ming-Hwa LMH, Li CW, Kuo CF. Halo-Substituted Chalcones and Azachalcones-Inhibited, Lipopolysaccharited-Stimulated, Pro-Inflammatory Responses through the TLR4-Mediated Pathway. Molecules. 2018;23:597.
22. Neto RAM, Santos CBR, Henriques SVC, Machado LO, Cruz JN, Silva CHTP, et al. Novel chalcones derivatives with potential antineoplastic activity investigated by docking and molecular dynamics simulations. J Biomol Struct Dyn. 2022;40:2204-2216.
23. Lee YS, Lim SS, Shin KH, Kim YS, Ohuchi K, Jung SH. Anti-angiogenic and anti-tumor activities of 2'-hydroxy-4'-methoxychalcone. Biol Pharm Bull. 2006;29:1028-103.
24. Zhuang C, Zhang W, Sheng C, Zhang W, Xing C, Miao Z. Chalcone: A Privileged Structure in Medicinal Chemistry. Chem Rev. 2017;117:7762-7810.
25. Welday KS, Hailu GS, Taye DK. Design, Synthesis, Characterization and in vivo Antidiabetic Activity Evaluation of Some Chalcone Derivatives. Drug Des Devel Ther. 2021;15:3119-3129.
26. Prelog V. Untersuchungen über assimétrica Synthesen I. Über den sterischen Verlauf der Reaktion von α-Ketosäure-esttern optisch activer Alkohole mit Grignard 'schen Verbindungen. Helvetica Chimica Acta. 1953;36:308-319.
27. Kaewin S, Poolsri W, Korkut GG, Patrakka J, Aiebchun T, Rungrotmongkol T, et al. A sulfonamide chalcone AMPK activator ameliorates hyperglycemia and diabetic nephropathy in db/db mice. Biomed Pharmacother. 2023;165:115158.
28. Acho LDR, Oliveira ESC, Carneiro SB, Melo FPA, Mendonça LS, Costa RA, et al. Antidiabetic Activities

and GC-MS Analysis of 4-Methoxychalcone. Applied Chem. 2024;4:140-156.
29. Cabrera M, Simoen M, Falchi G, Lavaggi ML, Piro OE, Castellano EE, et al. Synthetic chalcones, flavanones, and flavones as antitumoral agents: biological evaluation and structure-activity relationships. Bioorg Med Chem. 2007;15:3356-3367.
30. Iftikhar S, Khan S, Bilal A, Manzoor S, Abdullah M, Emwas AH, et al. Synthesis and evaluation of modified chalcone based p53 stabilizing agents. Bioorg Med Chem Lett. 2017;27: 4101-4106.
31. Melo CP, Pimenta M. Nanociência e Nanotecnologia. Brasília (DF). Revista Parcerias Estratégicas. 2004;18:9-21.
32. Fessi H, Puisieux F, Devissaguet JPh, Ammoury N, Benita S. Nanocapsule formation by interfacial polymer deposition following solvent displacement. Int J Pharm. 1989;55:R1-R4.
33. Dimer FA, Friedrich RB, Beck RCR, Guterres SS. Impacts of nanotechnology on health: production of medicines. Quim Nova. 2013;36:1520-1526.
34. Acácio BR, Robles VB, Prada AL, Assis JM, de Souza TP, Keita H, et al. Kollicoat MAE® 100P as a film former polymer for nanoparticles preparation. Rev Colomb Cienc Quím Farm. 2022;51:1215-1231.
35. Oliveira ESC, Acho LDR, Morales-Gamba RD, Rosário AS, Barcellos JFM, Lima ES, et al. Hypoglycemic effect of the dry leaf extract of Myrcia multiflora in streptozotocin-induced diabetic mice. J Ethnopharmacol. 2023;307:116241.
36. Ahmed M, Ahmed S. Functional, Diagnostic and Therapeutic Aspects of Gastrointestinal Hormones. Gastroenterol Res. 2019;12:233-244.
37. Ohkawa H, Ohishi N, Yagi K. Assay for lipid peroxides in animal tissues by thiobarbituric acid reaction. Bioquímica Anal. 1979;95:351-358.
38. Gomes MDB. Glitazones and metabolic syndrome: mechanisms of action, pathophysiology and therapeutic indications. Arquivos Brasileiros de Endocrinologia & Metabologia. 2006;50:271-280.
39. Owens IDE, Peppas NA. Opsonization, biodistribution, and pharmacokinetics of polymeric nanoparticles. Int. Journal of Pharm. 2006;307:93-102.
40. Kulkarni SA, Feng SS. Effects of Particle Size and Surface Modification on Cellular Uptake and Biodistribution of Polymeric Nanoparticles for Drug Delivery. Pharmaceutical Research. 2013;30:2512-2522.
41. Zeta Meter, Inc. Potencial Zeta: Um Curso Completo em 5 Minutos. available in http://www.zeta-meter.com
42. Han Y, Lee SH, Lee IS, Lee KY. Regulatory effects of 4-methoxychalcone on adipocyte differentiation through PPARγ activation and reverse effect on TNF-α in 3T3-L1 cells. Food Chem Toxicol. 2017;106:17-24.
43. Legrand P, Barratt G, Mosqueira V, Fessi H. Devissaguet JP. Polymeric nanocapsules as drug delivery systems. S.T.P. Pharma sciences. 1999;9:411-418.
44. Neto SF, Prada AL, Acho LDR, Torquato HFV, Lima CS, Paredes-Gamero EJ, et al. α-amyrin-loaded nanocapsules produce selective cytotoxic activity in leukemic cells. Biomed Pharmacother. 2021;139:111656.
45. Valencia MS. Synthesis and characterization of nanoparticles containing polyphenols with potential application in the food industry [PhD Thesis]. Pernambuco: Federal University of Pernambuco: 2020.
46. Patel P, Obrigado A, Kapoor DU, Prajapati BG. QbD decorated ellagic acid loaded polymeric nanoparticles: Factors influencing desolvation method and preliminary evaluations. Nano-Structures & Nano-Objects, 2024;40:101378.
47. Shahsavani D, Kazerani HR, Kaveh S, Gholipour-Kanani H. Determination of some normal serum parameters in starry sturgeon (Acipenser stellatus Pallas, 1771) during spring season. Comp Clin Path. 2010;19:57-61.
48. Young JF, Stagsted J, Jensen SK, Karlsson AH, Henckel P. Ascorbic acid, alpha-tocopherol, and oregano supplements reduce stress-induced deterioration of chicken meat quality. Poultry Science. 2003;82:1343-1351.
49. Cotinguiba GG, Silva JRN, de Sá Azevedo RR, Rocha TJM, dos Santos AF. Método de avaliação da defesa antioxidante: uma revisão de literatura. Journal of Health Sciences. 2013;15:231-237.
50. American Diabetes Association. 2. Diagnosis and Classification of Diabetes: Standards of Care in Diabetes—2024. Diabetes Care. 2024;47(Supplement 1):S20-S42.
51. Sociedade Brasileira de Diabetes. Diretrizes da Sociedade Brasileira de diabetes 2023-2024. São Paulo: Editora Clannad. 2023; 65.
52. Marshall RH, Eissa M, Bluth EI, Gulotta PM, Davis NK. Hepatorenal index as an accurate, simple, and effective tool in screening for steatosis. AJR Am J Roentgenol. 2012;199:997-1002.